ChemComm

Dynamic Article Links

Cite this: *Chem. Commun.*, 2012, **48**, 4866–4868

www.rsc.org/chemcomm

COMMUNICATION

Simultaneous detection of enterovirus 71 and coxsackievirus A16 using dual-colour upconversion luminescent nanoparticles as labels†

Shijia Wu, Nuo Duan, Xiaoyuan Ma, Yu Xia, Ye Yu, Zhouping Wang* and Hongxin Wang

Received 5th January 2012, Accepted 20th March 2012
DOI: 10.1039/c2cc00092j

We highlight a novel fluorescence analysis for sensitive and selective detection of EV-71 and CV-A16 by combining labelling technology based on dual-colour upconversion fluorescence nanoparticles (UCNPs) with magnetic bioseparation and concentration technology based on magnetite nanoparticles (MNPs).

Simple, novel and direct analysis or monitoring of significant viruses in complex biological samples is important for many biological studies and clinical diagnoses. Currently, combining nanomaterials and biomolecular recognition units is promising for the development of novel clinical diagnostic techniques. To enhance detection sensitivity, many highly luminescent nanomaterials, such as semiconductor quantum dots (QDs),[1] lanthanide-doped particles[2] and fluorescent dye-doped silica nanoparticles,[3] have been introduced for biodetection. However, they have intrinsic limitations, including inherent toxicity and chemical instability, that limit their application for biological detection and medical diagnosis. Although these phosphors work well under laboratory conditions, an increase in their background signal may be noted in the presence of interfering biomolecules and other fluorescent organic molecules that can be excited by UV radiation and are commonly present in biological and environmental samples. The presence of such molecules lowers the sensitivity of detection.[4] In addition, organic fluorescent dye-doped nanoparticles cannot be applied to the simultaneous detection of multiple analytes because different emission wavelengths are excited by different excitation. In comparison with the traditionally used downconversion with fluorescent biolabels, upconversion nanoparticles (UCNPs) exhibit unique luminescent properties, including the ability to convert longer wavelength radiation to shorter wavelength fluorescence *via* a two-photon or multi-photon mechanism,[5,6] high quantum yields, narrow emission peaks, large Stokes shifts, high chemical stability, and low toxicity.[7] No other material possesses this capability for upconversion anti-Stokes photoluminescence at conventional excitation light intensities. Additionally, the phosphor emission can be measured entirely free of autofluorescence and scattered excitation light, enabling bioassays with low background fluorescence signals. UCNPs also allow for tunable optical properties by varying the lanthanide dopants (*e.g.*, Tm, Er, and Ho) and the host matrix[7] used in their synthesis. By varying the combination of dopant ions, host materials and the concentration of the dopant ions, the emission wavelength and relative intensity of the emission peaks can be effectively controlled to modulate the emission colours of the lanthanide-doped UCNPs. Based on multicolour fine-tuning in the visible spectrum, they can be applied to simultaneous multiplexed biological labelling.

In contrast with time-consuming amplification procedures such as PCR, magnetic nanomaterials have been used extensively in the development of highly efficient magnetic concentration and bioseparation techniques.[8–10]

Hand, foot and mouth disease (HFMD) is normally mild but can have life-threatening manifestations. The spread of the disease is explosive and extensive, and HFMD has been recognised as a serious international public health problem. A series of large HFMD epidemics in the Asia–Pacific region, southeast Asia and China have been described that were associated with a rapid fulminant course. Smaller outbreaks have also been described in Europe.[11] The symptoms of HFMD, primarily affecting infants and children of less than 10 years of age, are characterised by fever, vesicular eruptions in the mouth and/or a rash sometimes accompanied by blisters.[12] The two primary etiologic agents of HFMD are Enterovirus 71 (EV-71) and Coxsackievirus A16 (CV-A16).[13,14]

Because the clinical symptoms of EV-71- and CV-A16-associated HFMD are similar, diagnosis depends largely on virus isolation and serotyping.[15] Using a conventional reverse transcriptase PCR (RT-PCR) strategy, specific detection of EV71 or CV-A16 has been reported.[16,17] However, the RT-PCR process is time consuming, and the risk of cross-contamination is increased with this approach. Therefore, the need exists to develop a rapid and reliable method for the detection of this causative agent to limit the extension of HFMD outbreaks.

In this study, we have described the preparation of surface-modified nanoparticles and constructed a homogeneous sandwich hybridisation assay based on upconversion fluorescence and magnetic bioseparation, which quantifies the two different DNAs of EV-71 and CV-A16 simultaneously by utilising the two distinct emission bands of the $NaYF_4$:Yb and Er/Tm UCNPs at 477 nm and 660 nm, respectively. To the authors's knowledge, this work is the first example in which multicolour

State Key Laboratory of Food Science and Technology, School of Food Science and Technology, Jiangnan University, Wuxi 214122, China. E-mail: wangzp@jiangnan.edu.cn; Fax: +86 510 85917023; Tel: +86 510 85917023

† Electronic supplementary information (ESI) available. See DOI: 10.1039/c2cc00092j

nanoparticles and magnetic bioseparation are used for EV-71 and CV-A16 detection.

The luminescent efficiency of these upconversion materials is known to be greatly dependent on the excited-state dynamics of the rare-earth ions and their interactions with the host matrix.[18] Ideal host materials should also have low lattice phonon energies, which are required to minimise non-radiative loss and maximise the radiative emission.[7] Therefore, the upconversion performance of these materials can be significantly enhanced with the suitable selection of a host matrix and by the selection of their phase. The upconversion luminescent nanomaterials used in this work are Yb, Er/Tm ion-pair doped hexagonal phase $NaYF_4$ nanoparticles. UCNPs were synthesised using hydrothermal techniques.[19] The optical spectrum, size and morphology of the bare and surface-modified UCNPs were characterised by fluorospectrophotometry (Fig. S1, ESI†), transmission electron microscopy (Fig. S2, ESI†), X-ray diffraction (Fig. S3, ESI†) analysis, and infrared spectroscopy (see Fig. S4, ESI†).

The amine-functionalised magnetic nanoparticles (MNPs) applied in this research were prepared using a one-pot synthesis technique. TEM (Fig. S5a, ESI†), FT-IR (Fig. S5b, ESI†) and XRD (Fig. S5c, ESI†) were demonstrated to characterise the as-synthesised magnetic nanoparticles (see, ESI†).

With magnetic-field-assisted separation and concentration technology, these magnetic and upconversion luminescent nanoparticles, bioconjugated with oligonucleotides, were used for the sensitive detection of trace amounts of DNA according to the procedure schematically depicted in Fig. 1. In a typical experiment for DNA detection, avidin-conjugated nanoparticles were specifically bonded to biotin-modified oligonucleotides, and a three-component sandwich assay was used.

The avidin-conjugated UCNPs were linked to the probe DNA and used as probes to monitor the presence of the specific target DNA strands. Meanwhile, the avidin-conjugated MNPs were linked to the capture DNA and incubated overnight at 37 °C. Then, the capture-DNA modified MNPs were hybridised with the target DNA for 1 h at 37 °C and washed three times.

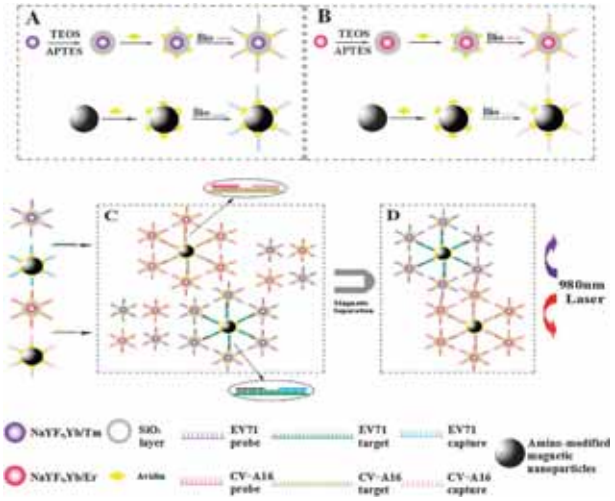

Fig. 1 Schematic diagram of the three-component sandwich assay method combining UCNP fluorescence with magnetic separation. The nanocomposite was purified with magnetic separation and detected with $NaYF_4$:Yb, Er/Tm UCNP fluorescence respectively. The excitation light was generated by a commercially available 980 nm laser.

This technique was then combined with a magnetic separation technique to remove the unreacted and nonspecifically bound targets. Following these procedures, probe DNA (the modified UCNP solution) was added and incubated for another hour to allow hybridisation with the overhanging region of the target DNA. The nanocomposite consisting of the magnetic and luminescent nanomaterials through matched DNA was then washed and magnetically separated. The trace amounts of DNA were detected by recording the upconversion luminescence intensity of the nanocomposite solution.

In a typical experiment, DNA3 and DNA6 (EV-71 target and CV-A16 target, respectively) of varying concentrations were added to the corresponding oligonucleotide (EV-71 capture and CV-A16 capture) in a modified magnetic nanoparticle solution (0.1 mg ml^{-1}) and incubated at 37 °C for 1 h. Afterwards, the DNA probes (EV-71 probe- and CV-A16 probe-modified UCNP solution) were combined and incubated for another hour to effect hybridisation with the overhanging region of the complementary target sequence. Then, the resultant nanocomposites were treated with magnetic separation and rising to remove the unhybridised probes. During each rising step, the nanoparticles were separated from the supernatant by the use of magnetic force. The nanocomposite was then redispersed in 0.1 M PBS for fluorescence analysis (Fig. 2). The nanocomposite luminescence spectra and intensities were examined using an F-7000 fluorescence spectrophotometer equipped with a 980 nm laser as the excitation light source. We chose the emission wavelengths of 477 nm and 660 nm to monitor the signals of the EV-71 target and CV-A16 target, respectively, such that the two emission peaks could not interfere with each other.

Based on this principle, without the implementation of PCR technology, the relative amounts of DNA3 and DNA6 were detected by employing the sandwich-type system consisting of a probe of DNA-conjugated UCNPs and the capture of DNA-conjugated magnetic nanoparticles. As shown in Fig. 3a, when the analytes (DNA3 and DNA6) were added into the sandwich-type system, the luminescence of $NaYF_4$:Yb, Er/Tm UCNPs gradually increased because when more target DNA was added, more probe DNA (conjugated UCNPs) and capture DNA (conjugated MNPs) were hybridised together. Therefore, more UCNPs can be collected by the assistant magnetic field.

As shown in Fig. 3b, the concentration of the target DNA (EV71) is shown to be in the range of 0.05–10 nM and is linear to the UC luminescence intensities. The linear calibration equation, $FUC = 38.745C + 13.501$ (FUC is the upconversion fluorescence intensity, C is the concentration of the target DNA (EV71), $R^2 = 0.9971$), of the detection was obtained according

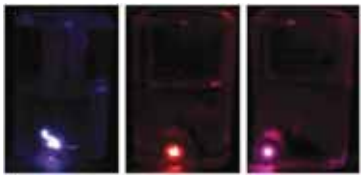

Fig. 2 Upconversion fluorescence with a 980 nm laser (down) images of a UCNP–MNP nanocomposite. $NaY_{0.78}F_4$:$Yb_{0.20}$, $Tm_{0.02}$ UCNP–MNP nanocomposite (left), $NaY_{0.28}F_4$:$Yb_{0.70}$, $Er_{0.02}$ UCNP–MNP nanocomposite (middle), mixture of $NaY_{0.78}F_4$:$Yb_{0.20}$, $Tm_{0.02}$ UCNP-MNP and $NaY_{0.28}F_4$:$Yb_{0.70}$, $Er_{0.02}$ UCNP–MNP nanocomposites (right).

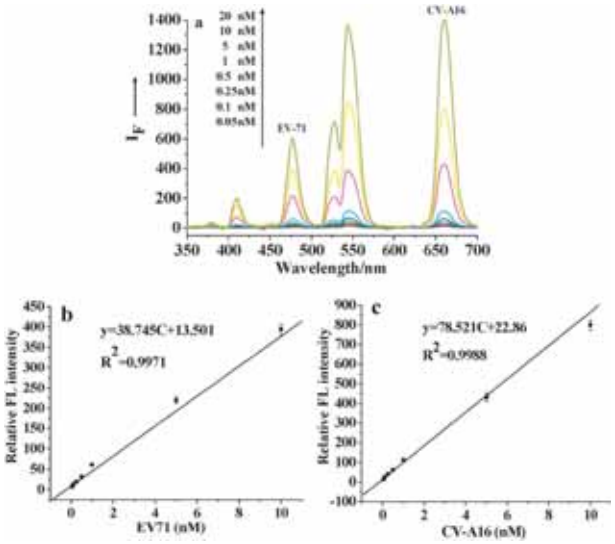

Fig. 3 (a) Fluorescence spectra of binary nanocomposites in the presence of different concentrations of target DNA, (b) the linear relationship between luminescence intensity and target DNA EV71, and (c) the linear relationship between luminescence intensity and target DNA CV-A16.

to the general detection procedure. Accordingly, Fig. 3c shows the linear relationship between the relative intensity of the UC luminescence and the concentration of the target DNA CV-A16. The intensity of the upconversion luminescence varied linearly with the concentration of the target DNA CV-A16 in the solution between 0.05 nM and 10 nM. The linear calibration equation was FUC = 78.521C + 22.86 (C is the concentration of the target DNA CV-A16, R^2 = 0.9988).

Statistical analysis reveals that the detection limit (DL) of the concentrations of target DNA EV71 and target DNA CV-A16 are 20 pM and 25 pM (3σ), respectively. The precision expressed as the relative standard deviation (RSD) of the target DNA EV71 detection is 2.61% (obtained from a series of 7 standard samples with each containing 1 nM of target DNA EV71). The RSD of DNA CV-A16 detection is 3.52%.

We tested the performance of the proposed UCNP-labelled method by measuring different concentrations of PCR products amplified from EV71 and CV-A16 DNA, which were extracted from human plasma samples freshly obtained from the Wuxi Disease Prevention and Control Center. The sensitivity of the assay was evaluated using 10-fold serial dilutions of PCR products of EV71 and CV-A16, respectively. The assayed results are summarised in Table S2 (see ESI†). Clinical evaluation of the proposed method was undertaken using a collection of 8 clinical specimens. The results revealed 7 samples positive for EV71 and 5 samples positive for CV-A16. EV71 was not detected in 1 sample, and CV-A16 was not detected in 3 samples. These results were consistent with the clinical diagnosis method (real-time PCR) obtained from the Wuxi Disease Prevention and Control Center. Recovery experiments of the calibrator for EV71 and CV-A16 from enhanced human plasma samples also indicated the excellent accuracy and precision of the proposed method (Table S3, see ESI†).

In conclusion, this report describes a novel and sensitive analytical method for simultaneously detecting EV71 and CV-A16 based on a sandwich-type method developed using capture DNA immobilised on the surface of MNPs and probe DNA immobilised on the surface of UCNPs. Combined with the standard curves, the assay was applied successfully for the quantitative analysis of viral loads in clinical samples with EV71 or CV-A16. As the biosensors consisted of the nanocomposite, the use of MNPs provided rapid separation and concentration, and the multicolour UCNPs had tunable optical properties without autofluorescence. Given its sensitivity and rapid detection, we believe that this approach has the potential to be a widely used technology for the detection of viruses in clinical diagnostic analyses. In future studies, related applications and further conformation of the multicolour UCNPs will be investigated by our group.

This work was partly supported by National S&T support program of china (2012BAK08B01, 2011BAK10B03), Science and Technology Supporting Project of Jiangsu Province (BE2010679, BE2011621), Research Fund for the Doctoral Program of Higher Education (20110093110002), CIQ Project 2012IK166, and NCET-11-0663.

Notes and references

1 Z. A. Peng and X. G. Peng, *J. Am. Chem. Soc.*, 2001, **123**, 183–184.
2 F. Meiser, C. Cortez and F. Caruso, *Angew. Chem., Int. Ed.*, 2004, **43**, 5954–5957.
3 S. Santra, H. Yang, D. Dutta, J. T. Stanley, P. H. Holloway, W. H. Tan, B. M. Moudgil and R. A. Mericle, *Chem. Commun.*, 2004, 2810–2811.
4 L. Y. Wang and Y. D. Li, *Chem. Commun.*, 2006, 2557–2559.
5 F. Auzel, *Chem. Rev.*, 2004, **104**, 139–173.
6 X. Wang and Y. D. Li, *Chem. Commun.*, 2007, 2901–2910.
7 F. Wang and X. G. Liu, *Chem. Soc. Rev.*, 2009, **38**, 976–989.
8 H. W. Gu, P. L. Ho, K. W. T. Tsang, C. W. Yu and B. Xu, *Chem. Commun.*, 2003, 1966–1967.
9 J. M. Nam, C. S. Thaxton and C. A. Mirkin, *Science*, 2003, **301**, 1884–1886.
10 L. Y. Wang, J. Bao, L. Wang, F. Zhang and Y. D. Li, *Chem.–Eur. J.*, 2006, **12**, 6341–6347.
11 J. R. Wang, Y. C. Tuan, H. P. Tsai, J. J. Yan, C. C. Liu and I. J. Su, *J. Clin. Microbiol.*, 2000, **40**, 10–15.
12 M. J. Cardosa, D. Perera and B. A. Brown, *Emerging Infect. Dis.*, 2003, **9**, 461–468.
13 B. A. Brown, M. S. Oberste, J. P. Alexander, M. L. Kennett and M. A. Pallansch, *J. Virol.*, 1999, **74**, 9969–9975.
14 L. Y. Chang, T. Y. Lin, Y. C. Huang, K. C. Tsao, S. R. Shih, M. L. Kuo, H. C. Ning, P. W. Chung and C. M. Kang, *Pediatr. Infect. Dis. J.*, 1999, **18**, 1092–1096.
15 K. A. Lim and M. Benyesh-Melnick, *J. Immunol.*, 1960, **84**, 309–317.
16 W. A. Nix, M. S. Oberste and M. A. Pallansch, *J. Clin. Microbiol.*, 2006, **44**, 2698–2704.
17 K. C. Tsao, P. Y. Chang, H. C. Ning, C. F. Sun, T. Y. Lin, L. Y. Chang, Y. C. Huang and S. R. Shih, *J. Virol. Methods*, 2002, **102**, 9–14.
18 J. H. Zeng, J. Su, Z. H. Li, R. X. Yan and Y. D. Li, *Adv. Mater.*, 2005, **17**, 2119–2123.
19 L. Y. Wang, R. X. Yan, Z. Y. Hao, L. Wang, J. H. Zeng, J. Bao, X. Wang, Q. Peng and Y. D. Li, *Angew. Chem., Int. Ed.*, 2005, **44**, 6054–6057.

